Available online at www.sciencedirect.com
SCIENCE DIRECT®
International Journal of Coal Geology xx (2005) xxx–xxx
International Journal of COAL GEOLOGY
www.elsevier.com/locate/ijcoalgeo

Electromagnetic radiation induced by mining rock failure

V. Frid[a,*], K. Vozoff[b]

[a]*Geological and Environmental Sciences, Ben Gurion University of the Negev, Beer Sheva, Israel 84105*
[b]*Department of V&A Geoscience, POB 996 Spit Junction, NSW Australia 2088*

Received 12 March 2004; received in revised form 6 July 2004; accepted 2 March 2005

Abstract

Anticipating roof fall in mine workings has been a problem for centuries. The focus in the search for early warning indicators has been on observing seismic (acoustic) events prior to the fall. These precursors have been studied in great detail at many places, but none has been fully successful. So far, no valid, effective early warning system based on low-frequency seismic precursors has been established. In this paper, we investigated a promising new technique, which is not yet completely understood or been widely tested in mines. The new method is the sensing of the embryonic stages of roof fall by detection of high frequency electromagnetic radiation (EMR) emitted from rock microcracks. Two examples of combined observations of EMR and low frequency acoustic emission prior to roof fall at Moonee Colliery are presented. Anomalously, high EMR was detected more than 1 h before roof fall, giving a significant time advantage over the first indicators of low frequency acoustic emission. Analysis of Benioff strain release diagrams of EMR emanating from developing medium scale failure in the mine enabled us to fill the 'gap' between previously known microscale (rock fracture in lab) and macroscale (earthquake) EMR observations, and to conclude that indeed a common fundamental relationship must lie behind this multi-scale phenomenon.

Keywords: Mining; Hazards; Collapse; Electromagnetic radiation; Risk

1. Introduction

Australian longwall mines currently use microseismic monitoring to provide some warning of an imminent occurrence of roof failure, windblast, or gas outburst from wall. Microseismic monitoring detects acoustic emissions resulting from microfracturing in stressed zones. The method requires (i) sensors to be coupled to the mine strata, (ii) long cables run to intrinsically safe (IS) recording equipment, and (iii) signals filtered to reject ambient acoustic noise. Systems currently in use are not easily moved, often produce false alarms, and/or fail to provide sufficient warning time for remedy.

An alternative system that could be used to predict outburst and gas-out is monitoring of electromagnetic radiation (EMR) that (like acoustic emission) is also generated from fracturing, although its detection does

* Corresponding author.
E-mail address: vfrid@bgumail.bgu.ac.il (V. Frid).

0166-5162/$ - see front matter © 2005 Elsevier B.V. All rights reserved.
doi:10.1016/j.coal.2005.03.005

not require physical contact with the rock strata. Most experience with this method has been in Russian mines of several kinds (but primarily collieries) where roadways are routinely traversed with a hand-held detector at a distance of approximately one half meter from the wall. Attenuation of the electromagnetic (EM) signal in air would be negligible. Signal reduction would be geometric, depending on the lateral extent of the source region, so signal should be detectable many meters away from the wall for a source region of (typically) 10 m extent. The present paper describes the results of demonstration measurements in one colliery. They extend and corroborate the results previously obtained in Russian mines as described by Frid (1997a,b) and supported by laboratory measurements in many countries (see below). A new commercial instrument was recently announced by the laboratory (VNIMI, St Petersburg, Russia) which developed the method.

EMR investigations conducted on different materials, and sometimes combined with measurements of acoustic emission, showed that EMR was indeed induced by the microcracks. The materials tested included metals and alloys (Misra, 1975; Jagasivamani and Iyer, 1988), single crystals (Gol'd et al., 1975; Khatiashvili, 1984), various rock types (Nitsan, 1977; Warwick et al., 1982; Ogawa et al., 1985; O'Keefe and Thiel, 1995; Rabinovitch et al., 1995, 1996, 1998, 2000; Goncharov et al., 1980; Sobolev et al., 1982; Cress et al., 1987; Yamada et al., 1989; Frid, 1990), and ice (Fifolt et al., 1993; Petrenko, 1993; O'Keefe and Thiel, 1996). From an analysis of all available data on fracturing, Frid et al. (2003) concluded that EMR amplitude is determined by elasticity, strength of (inter-ionic) bonds cut by fracturing, and crack area. Confining stress has an effect through its effect on elasticity (Frid, 1999).

Numerous large scale field investigations showed that the magnitude of EMR sharply increased several hours or even days before an earthquake and quickly decreased at its onset or immediately before (Sadovskii et al., 1979; Gokhberg et al., 1979, 1982, 1985, 1986; Morgunov, 1985; Gershenzon et al., 1987; Yoshino and Tomizawa, 1989; Yoshino et al., 1993). The magnitude of the detected EMR anomalies was up to 10–15 dB above the usual noise level. Analysis of 60 earthquake events concluded that EMR was a "short-term" precursor, with an estimated mean time prior to an earthquake of ~ 6 h (Rikitake, 1997). It is now understood that EMR is a phenomenon associated with multi-scale fracturing. New evidence indicates that its behavior can be described in terms of fractal electrodynamics (Eftaxias et al., 2004).

Medium-scale EMR studies in mines are rare. Nesbitt and Austin (1988) detected EMR in a gold mine (2.5 km depth). An EMR signal (1.2 mA/m amplitude) was generated several seconds prior to the microseismic event (magnitude of −0.4). Recording of EMR activity in Ural bauxite mines showed that its values sharply increased with rockburst hazard increase (Scitovich and Lazarevich, 1985). Analogous works in the Noril'sk polymetal deposit (Krasnoyarsk region) revealed an increase of EMR amplitude (up to 150–200 mV/m) and activity in the rockburst prone zones (Red'kin et al., 1985). Markov and Ipatov (1986) investigated EMR activity changes in an underground apatite mine (Khibin deposit, Kola peninsula) and found that EMR amplitude in rockburst hazardous zones was in the range of 8–25 mV/m and EMR activity there was significantly higher than the normal noise level. Frid (1997a,b, 2000, 2001) observed EMR anomalies before rockbursts and gas outbursts in coal mines and presented systematic criteria for their use.

The aim of this paper is to demonstrate the potential of EMR monitoring as a viable forewarning system of developing failure. Analytical arguments are necessarily semiquantitative, as is often the case when describing poorly understood physical phenomena.

2. Equipment and experimental site

The investigation was conducted at the Moonee Colliery, about 100 km north of Sydney, Australia, which had a problem with windblasts and used an acoustic emission system for warning.

Magnetic loop antennas were about 400 mm square and 20 mm thick (Fig. 1). They were contained in a tough plastic fabric 'envelope' to which were attached nylon (seat belt material) straps, 1 m long, with metal loops at each end, so they could be bolted to the rib as a safety precaution in case of windblast. Loop properties (inductance, resistance and capacitance) were within the values permitted for the IS approvals. They were connected to the recorder through a passive bandpass (L–R) filter by a 5 m cable. The filter was

Fig. 1. Magnetic loop antenna (at the right) and EMR recorder.

designed for anti-aliasing and to reject low frequency machinery noise. The IS recorders were robust PCs designed for in-seam seismic and other underground data acquisition. Hard disk drives (10 GB) and preamplifiers (*1, *5, and *30 gain) were installed to boost the signals from the loops. The high speed input channel of each was capable of A/D conversion at 100 kHz. This permitted a maximum frequency of 50 kHz. Mine requirements mandated that the PCs were operated in a flameproof box.

3. Recording method

Due to presence of machinery noise, we wished to perform most EMR measurements during hydrofracturing operations, when mining had ceased and noise would be least. In each instance, the sensing loop was mounted around the corner from the maingate in the nearest cut-through, typically around 50 m from the centre of the working face (Fig. 2 shows the experimental setup).

When the loop had been installed, the system recorded data until the battery had discharged, 8–10 h later. The software recorded a sequence of binary records, paused for ~ 10 s for reinitialization, then went to the next record. The experimental data were transferred to a CD writer. The binary data were converted to ASCII for examination, processing, plotting, and analysis. Each binary file was just over 1 MB long. The ASCII files were approximately 4 MB in size, each containing 540,600 data points. A single recording session gave about 7000 such files.

4. Description of the data

We present results of two combined EMR and acoustic emission observations prior to roof fall that were recorded on 15 June and 5 July 2002. The 15 June session began following unsuccessful hydrofracturing and recorded through a subsequent roof fall. The 5 July session was intended to record during routine mining, although a small fall occurred as it was recording. Table 1 lists record details.

Fig. 3a shows a short fragment of an EMR record. Time- and frequency-analysis of our records showed that their decay characteristics are very similar to those measured by Rabinovitch et al. (2002a) during blasting and drilling (Fig. 3b,c) where EMR records consisted of numerous individual pulses. Typical EMR pulses induced by a single crack are shown in Fig. 3d. The FFT of all observed EMR sequences shows that the most energetic part of the EMR spectrum lies in the frequency range between 25 and 50 kHz. As was shown by Frid et al. (2003), the frequency of EMR signals is inversely proportional to the fracture width $b = V_R / 2f$, where V_R is the Rayleigh wave speed and f is the EMR frequency. Assuming a (typical) Rayleigh wave speed of 1000 m/s enables us

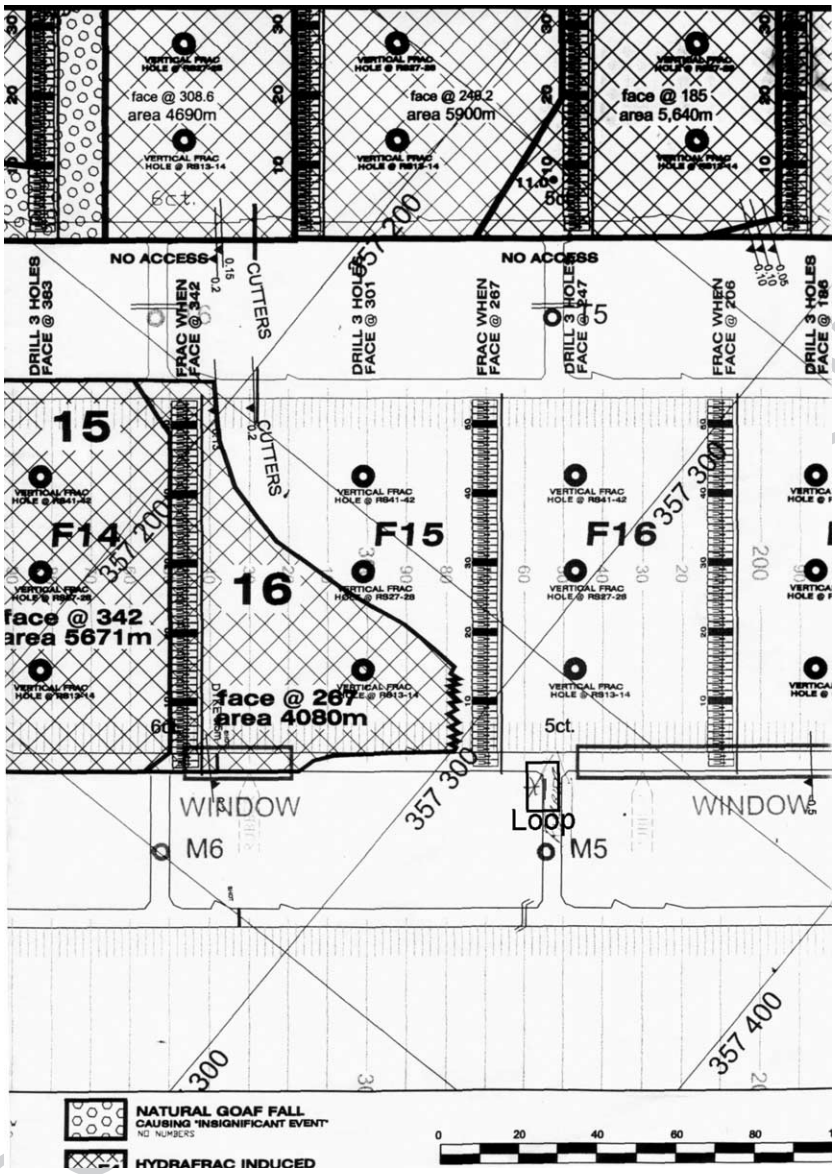

Fig. 2. EMR recorder near mine face with EMR antenna (denoted by the "loop") about 50 m from it. Black circles indicate vertical hydrofrac drillholes; crosshatching shows roof fall without hydrofrac stimulation.

to define the range of the widths of the cracks causing our EMR signals to be 1–2 cm.

Frid (2001) showed that the zone affected by mining and characterized by the increased stress level could be estimated to be about 2.5 times its width in all directions. (This is a conservative approximation made by Frid (2001) on the basis of elastic behavior of a single underground opening under confining stress (Jaeger, 1964). Petukhov and Lin'kov (1983) show that geometric complications in openings will increase stress concentrations and the size of a highly stressed zone. This zone is the source of crack induced EMR.

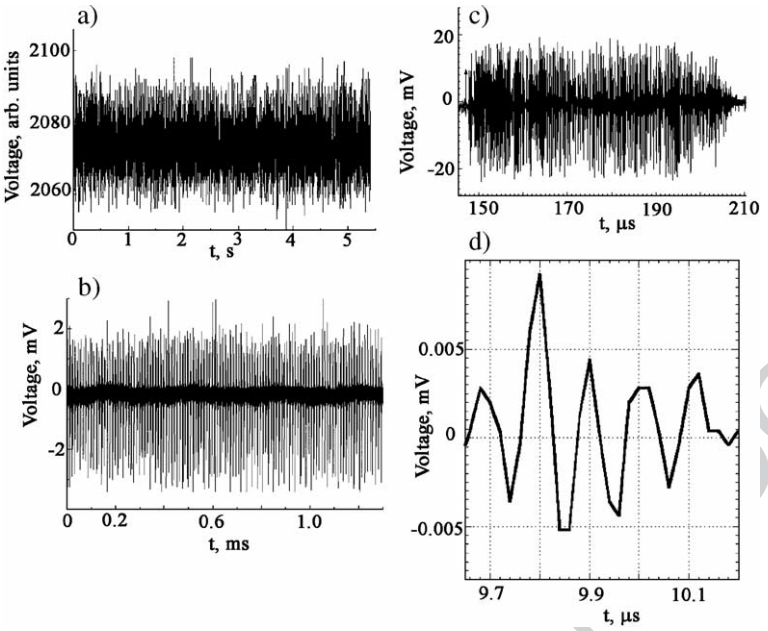

Fig. 3. EMR signals observed during: (a) mining, (b) blasting, (c) drilling, and (d) single EMR pulse induced by individual crack. Panels (b)–(d) from Rabinovitch et al. (2002a). Note change in time scale.

Assuming mine working width to be about 3 m, we can estimate the volume of this zone as $V=226$ m^3 per each 1 m of its length. Frid (2001) showed that crack number N created in highly stressed volume, V, could be estimated as follows: $N=V/(kc)^3$ (where $k=3$ is the concentration factor (Zurkov et al., 1969), and c is the crack length). For purposes of estimating N, the crack length can be taken to be equal to the crack width (1–2 cm). The validity of this assumption is based on the equivalence of theoretical and experimental criteria for rockburst prediction (Frid, 2001). It enables us to estimate the number of cracks N inducing individual EMR pulses to be about 10^6 for every 1 m of mine working. This very large value explains the very dense character of our EMR record where overlapping individual pulses were obtained. Similar properties of EMR signals were investigated by Goldbaum et al. (2003), who showed that crack formation at time intervals shorter than EMR pulse duration excites EMR pulses which partially overlap or even coincide.

Fig. 4 shows first example of a combined measurement of acoustic emission and EMR prior to roof failure. As is seen, the roof fall (Richter magnitude was equal to 0) took place at 12:09:17. EMR mean values routinely increased up to 11:06:03, remained large up to 12:03:28, and decreased after the roof fall. Hence, the maximum in the mean of EMR activity was about 1 h before the maximum of acoustic emission (roof fall).

Fig. 5 shows a second example of the combined measurement of acoustic emission and EMR prior to roof failure, where the first two bursts of acoustic emission (Richter magnitude of which was −0.6, −0.8) were observed at 8:59:09, after which the acoustic emission level was in the range of its background (Richter magnitude of which was −2,

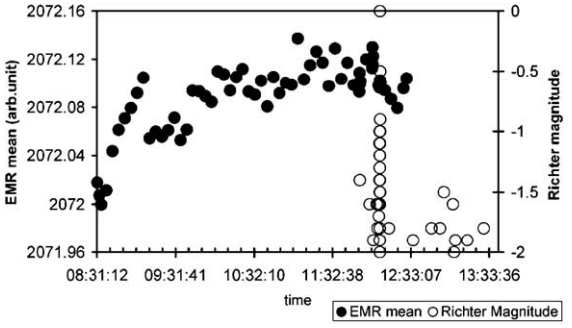

Fig. 4. The first example of combined EMR and acoustic emission recording prior to roof fall.

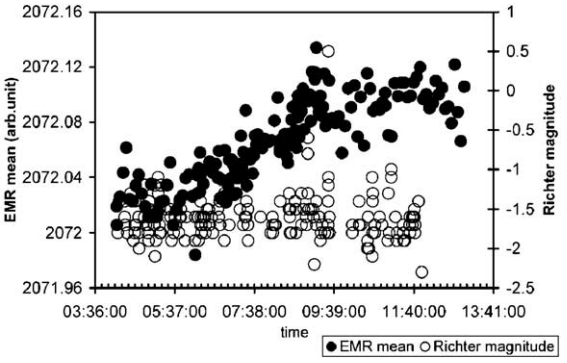

Fig. 5. The second example of combined EMR and acoustic emission measurement prior to roof fall.

−1). The maximum of acoustic emission magnitude (−0.5) coinciding with roof fall was recorded at 9:30:26. A comparison of acoustic emission data with EMR recordings showed that, at 7:17:35, about 1 1/2 h prior to the first small burst of acoustic emission, EMR activity became larger than its background level (see between 4:08 and 7:17) and reached its maximum at 9:11:56, i.e. ~ 19 min earlier than the acoustic emission peak.

Our results can be presented using a Benioff strain release diagram. The Benioff strain is defined as the square root of the energy of emitted signals. Based on their review of a large number of results, Jaume and Sykes (1999) concluded that changes in the Benioff strain release prior to earthquakes were equivalent to those observed in rock failure in the laboratory, and constitute an important feature of 'critical point' systems. Bufe and Varnes (1993) also showed that using the cumulative Benioff strain release leads to more accurate predictions of the time of major failure. Rabinovitch et al. (2002b), analyzing EMR amplitude changes induced by rock compression, showed a similarity in the fractal nature of the processes controlling EQs and those of EMR induced by rock fracture, and showed that

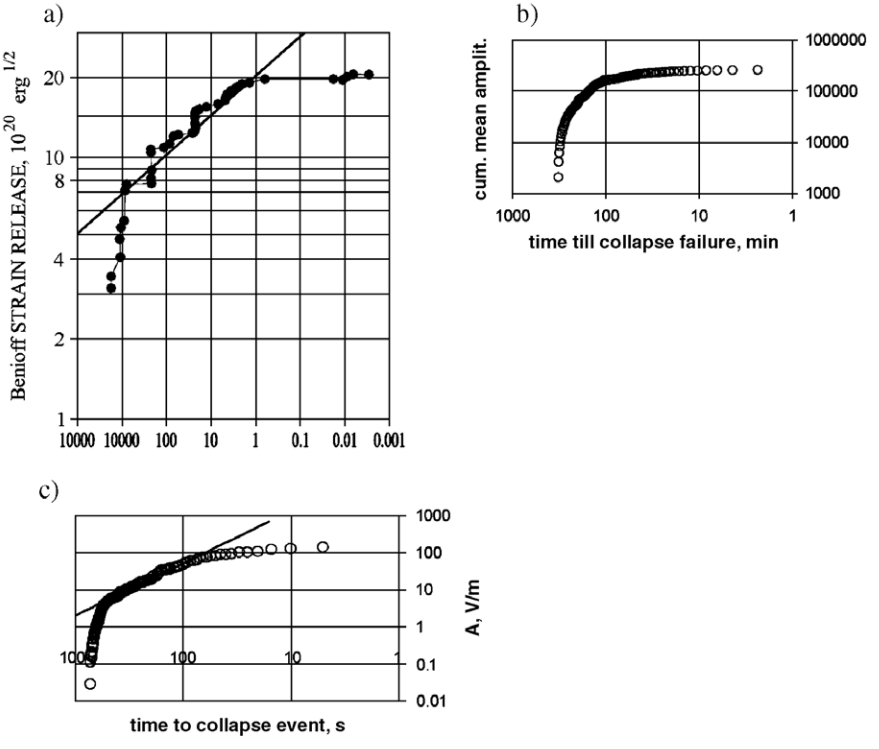

Fig. 6. Benioff strain release diagrams of panel (a) soft-γ radiation prior to very large-scale collapse (redrawn from Fig. 3 of Kossobokov et al., 2000), (b) EMR prior to roof fall, and (c) EMR during rock compression (Rabinovitch et al., 2002b).

amplitude of EMR pulses is the square root of the electromagnetic energy recorded. Hence, it could be used in place of Benioff strain.

We present the data on a bilogarithmic ('log–log') scale as was proposed by Kossobokov et al. (2000), where the x-axis measures the (reversed) "relative time" while the y-axis is cumulative Benioff strain release. Fig. 6a (redrawn from Fig 3 of Kossobokov et al., 2000) shows soft-γ radiation prior to very large-scale collapse. In such plots, the relative time of the collapse is 0, and equals 1 when the first event occurred. Fig. 6b shows a bilogarithmic strain release diagram of EMR signals recorded prior to roof fall.

A comparison of these diagrams with one presented by Rabinovitch et al. (2002b) (Fig. 6c) for EMR signals emanating during rock compression reveals qualitative similarity of the process underlying these phenomena on three different scales (large-EQ, medium-roof fall, and microrock compression in lab).

All three diagrams consist of three principal phases: nucleation, intermediate, and irreversible. During the nucleation phase, the graphs are almost vertical, during the intermediate phase, their slope is constant, and in the irreversible phase, the slope monotonically declines, inevitably ending with rock collapse. Our EMR measurements showed (Fig. 6b) that as early as 100 min before roof fall, the failure process had reached its irreversible part and hence rock collapse had been unavoidable.

As we noted above, first indications of acoustic emission leading up to the roof fall were 70 min later than first EMR precursors and only a half hour prior to the roof collapse itself.

To understand these results, note that rock destruction at all scale levels (from rock samples up to crust fracture) adhere to the following "sequence": nucleation of micro cracks, their accumulation, and coalescence ending in failure (Zurkov et al., 1969; Regel' et al., 1972; Kuksenko and Mansurov, 1986, 1987; Petrov and Gorobetz, 1987; Gueguen and Palciauskas, 1994; Mansurov, 1994; Rechez and Lockner, 1994; Rechez, 1999). As we understand it, EMR emanates from the very early onset of destruction, while the bulk of the low frequency acoustic emissions are mainly linked to the large-scale fracture itself (Frid et al., 2003). Hence, recording high frequency EMR excited by numerous microcracks (1–2 cm in width), nucleation of which begins much earlier than the roof fall itself, yields a significant time advantage for the early collapse warning.

Moreover, the time between crack nucleation and final failure has a tendency to increase as failure intensity increases (Kuksenko et al., 1982, 1987; Mansurov, 1994). Such behavior is known to be valid for laboratory fracture experiments, for pillar loading in mines, for rockbursts, and (on a still larger scale) even for earthquakes. Hence, the detection of EMR emanating from the failure enhances the time advantage as the collapse size increases. This conclusion is in agreement with many prior studies, viz:

- EMR was observed to be a short-term (~ 6 h) forecaster of 60 analyzed earthquakes (Rikitake, 1997),
- EMR was excited several hours or even days prior to large scale collapse (Gokhberg et al., 1979, 1982, 1986; Yoshino and Tomizawa, 1989),
- EMR signal was emitted ~ 500 μs before the acoustic emission signals during laboratory investigations of rock failure (O'Keefe and Thiel, 1995).

5. Summary and conclusions

1. EMR signals measured in mines are qualitatively similar to those measured in the laboratory during rock fracturing and in open quarries during blasting.
2. Analysis of fracture sizes showed that fractures of the order of 1–2 cm were the main source of measured EMR.
3. Comparison of the EMR and acoustic emission records showed that anomalous EMR activity had been measured much earlier than acoustic emission. An increase in the scale of failure (micro-medium-macro) increases the time advantage of EMR detection over acoustic detection.
4. Analysis of Benioff strain release diagrams of EMR records in the mine showed their similarity to those known for earthquakes and rock fracture. Similarity of mine-induced EMR to those of micro- and macroscale, together with analysis of sizes of cracks exciting EMR, enables us to conclude that EMR was generated during a crack nucleation phase prior to the incipient roof fall.

6. Uncited reference

Jaume and Sykes, 1996

Acknowledgements

The Moonee Colliery measurements were carried out under Project C9005 of the Australian Coal Association Research Program, with the encouragement and help of Richard Danell, John Doyle, John Edwards, Ross Gibson, Peter Hatherly, Lawrence Leung, Andrew Newland, Brian O'Neill, and Phil Wolfenden. Underground access was made possible by the colliery and its manager, Ross Campbell.

References

Bufe, C.G., Varnes, D.J., 1993. Predictive modeling of the seismic cycle in the Greater San Francisco Bay Region. J. Geophys. Res. 98, 9871–9983.

Cress, G.O., Brady, B.T., Rowell, G.A., 1987. Sources of electromagnetic radiation from fracture of rock samples in the laboratory. Geophys. Res. Lett. 14, 331–334.

Eftaxias, K., Frangos, P., Kapiris, P., Polygiannakis, J., Kopanas, J., Peratzakis, A., Skountzos, P., Jaggard, D., 2004. Model of preseismic electromagnetic emissions in terms of fractal-electrodynamics. Fractals 12 (2), 1–31.

Fifolt, D.A., Petrenko, V.F., Schulson, E.M., 1993. Preliminary study of electromagnetic radiation from cracks in ice. Philos. Mag., B 67 (3), 289–299.

Frid, V., 1990. Rockburst hazard forecast of coal seams by their electromagnetic radiation. PhD thesis, State Research Institute of Mining Geomechanics and Mine Surveying (VNIMI), S. Petersburg (in Russian).

Frid, V., 1997a. Rock-burst hazard forecast by electromagnetic radiation excited by rock fracture. J. Rock Mech. Rock Eng. 30 (4), 229–236.

Frid, V., 1997b. Electromagnetic radiation method for rock and gas outburst forecast. J. Appl. Geophys. 38, 97–104.

Frid, V., 1999. Electromagnetic radiation associated with induced triaxial fracture in granite. Philos. Mag. Lett. 79 (2), 79–86.

Frid, V., 2000. Electromagnetic radiation method water—infusion control in rockburst-prone strata. J. Appl. Geophys. 43, 5–13.

Frid, V., 2001. Calculation of electromagnetic radiation criterion for rockburst hazard forecast in coal mines. Pure Appl. Geophys. 158, 931–944.

Frid, V., Rabinovitch, A., Bahat, D., 2003. Fracture induced electromagnetic radiation. J. Phys., D 36, 1620–1628.

Gershenzon, N., Gokhberg, M., Morgunov, V., 1987. Sources of electromagnetic emissions preceding seismic events. Izv. Earth Phys. 23 (2), 96–101.

Gokhberg, M., Morgunov, V., Aronov, E., 1979. High frequency electromagnetic radiation during seismic activity. Dokl. Akad. Nauk SSSR 248, 1077–1081.

Gokhberg, M., Yoshino, T., Morgunov, V., 1982. Results of recording operative electromagnetic earthquake precursor in Japan. Phys. Solid Earth 18 (2), 144–146.

Gokhberg, M., Gufel'd, I., Gershenzon, N., 1985. Electromagnetic effects during rupture of the earth's crust. Phys. Solid Earth 21, 52–62.

Gokhberg, M., Morgunov, V., Matveyev, V., 1986. On the observation of anomalous electromagnetic emission in the epicentral zone of an earthquake. Phys. Solid Earth 22 (8), 676–678.

Gol'd, R.M., Markov, G., Mogila, P.G., 1975. Pulsed electromagnetic radiation of minerals and rocks subjected to mechanical loading. Phys. Solid Earth 7, 109–111.

Goldbaum, J., Frid, V., Bahat, D., Rabinovitch, A., 2003. An analysis of complex EMR signals induced by fracture. Meas. Sci. Technol. 14, 1839–1844.

Goncharov, A., Korjakov, V.P., Kuznetzov, V.M., 1980. Acoustic emission and electromagnetic radiation during uniaxial compression. Dokl. Akad. Nauk SSSR 255 (4), 821–824.

Gueguen, Y., Palciauskas, V., 1994. Introduction to the Physics of Rocks. Princeton University Press, Princeton.

Jaeger, J.C., 1964. Elasticity, Fracture and Flow, Second edition. Methuen and Company, London.

Jagasivamani, V., Iyer, K.J.L., 1988. Electromagnetic emission during the fracture of heat-treated spring steel. Mater. Lett. 6 (11–12), 418–422.

Jaume, S.C., Sykes, L.R., 1996. Evolution of modern seismicity in the San Francisco Bay Region, 1850 to 1993: seismicity changes related to the occurrence of large and great earthquakes. J. Geophys. Res. 101, 765–789.

Jaume, S.C., Sykes, L.R., 1999. Evolving towards a critical point: a review of accelerating seismic moment: energy release prior to large and great earthquakes. Pure Appl. Geophys. 155, 279–306.

Khatiashvili, N., 1984. The electromagnetic effect accompanying the fracturing of alkaline halide crystals and rocks. Phys. Solid Earth 20, 656–661.

Kossobokov, V.G., Keilis-Borok, V.I., Cheng, B., 2000. Similarities of multiple fracturing on a neutron star and on the earth. Phys. Rev., E 61 (4), 3529–3533.

Kuksenko, V.S., Mansurov, V.A., 1986. Fracture localization in rocks at different scale levels. Phys. Tech. Probl. Econ. Resour. Min. 3, 49–55.

Kuksenko, V.S., Lyashkov, A.I., Mirzoev, K.M., 1982. Connection between the sizes of cracks generated under loading and duration of elastic energy emission. Dokl. Akad. Nauk SSSR 246 (4), 846–848.

Kuksenko, V.S., Ingevatkin, I.E., Mahgikov, B.C., 1987. Physical and methodical foundations of rockburst forecast. Phys. Tech. Probl. Econ. Mater. Min. 1, 9–21.

Mansurov, V.A., 1994. Acoustic emission from failing rock behavior. Rock Mech. Rock Eng. 27 (3), 173–182.

Markov, G.A., Ipatov, Y., 1986. Method of electromagnetic radiation for rockburst forecast on apatite mines. Eng. Geol. 3, 54–57 (in Russian).

Misra, A., 1975. Electromagnetic effects at metallic fracture. Nature 254, 133–134.
Morgunov, V., 1985. Electromagnetic emission during seismic activity. Phys. Solid Earth 21 (3), 220–226.
Nesbitt, A.C., Austin, B.A., 1988. The emission and propagation of electromagnetic energy from stressed quartzite rock underground. Trans. S. Afr. Inst. Electr. Eng. 79, 53–57.
Nitsan, V., 1977. Electromagnetic emission accompanying fracture of quartz-bearing rocks. Geophys. Res. Lett. 4 (8), 33–336.
O'Keefe, S.G., Thiel, D.V., 1995. A mechanism for the production of electromagnetic radiation during fracture of brittle materials. Phys. Earth Planet. Inter. 89, 127–135.
O'Keefe, S.G., Thiel, D.V., 1996. Conductivity effects on electromagnetic emissions (EME) from ice fracture. J. Electrost. 36, 225–234.
Ogawa, T., Oike, K., Miura, T., 1985. Electromagnetic radiation from rocks. J. Geophys. Res. 90 (d4), 6245–6249.
Petrenko, V.F., 1993. On the nature of electrical polarization of materials caused by cracks. Application to ice electromagnetic radiation. Philos. Mag., B 67 (3), 301–315.
Petrov, V.A., Gorobetz, L.Z., 1987. Size effect of the concentration threshold of destruction. Phys. Solid Earth 23 (1), 75–77.
Petukhov, I.M., Lin'kov, L.M., 1983. Mechanics of Rock Bursts and Outbursts. Nedra, Moscow.
Rabinovitch, A., Bahat, D., Frid, V., 1995. Comparison of electromagnetic radiation and acoustic emission in granite fracturing. Int. J. Fract. 71 (2), r33–r41.
Rabinovitch, A., Bahat, D., Frid, V., 1996. Emission of electromagnetic radiation by rock fracturing. Z. Geol. Wiss. 24 (3–4), 361–368.
Rabinovitch, A., Frid, V., Bahat, D., 1998. Parameterization of electromagnetic radiation pulses obtained by triaxial fracture in granite samples. Philos. Mag. Lett. 77 (5), 289–293.
Rabinovitch, A., Frid, V., Bahat, D., Goldbaum, J., 2000a. Fracture area calculation from electromagnetic radiation and its use in chalk failure analysis. Int. J. Rock Mech. Min. Sci. 37, 1149–1154.
Rabinovitch, A., Bahat, D., Frid, V., 2002a. Similarity and dissimilarity of electromagnetic radiation from carbonate rocks under compression, drilling and blasting. Int. J. Rock Mech. Min. Sci. 39 (1), 125–129.
Rabinovitch, A., Frid, V., Bahat, D., 2002b. Gutenberg–Richter type relation for laboratory fracture induced electromagnetic radiation. Phys. Rev., E 65, 011401–011404.
Rechez, Z., 1999. Mechanisms of slip nucleation during earthquakes. Earth Planet. Sci. Lett. 170, 475–486.
Rechez, Z., Lockner, D.A., 1994. Nucleation and growth of faults in brittle rocks. J. Geophys. Res. 99, 18159–18173.
Red'kin, V., Kuprijanov, A.S., Bufalov, V.V., 1985. Geophysical devices for distance rock burst control. In: Smirnov, V. (Ed.), Geophysical Methods of Stress and Deformation Control. Novosibirsk, pp. 81–82 (in Russian).
Regel', V.R., Slutsker, A.I., Tomashevskii, E.E., 1972. The kinetic nature of the strength solids. Sov. Phys., Usp. 1, 45–65.
Rikitake, T.J., 1997. Nature of electromagnetic radiation precursory to an earthquake. Geomagn. Geoelectr. 49, 1153–1163.
Sadovskii, M.A., Sobolev, G.A., Migunov, N.I., 1979. Changes of natural radiowaves radiation during Karpatian earthquake. Dokl. Akad. Nauk SSSR 244 (2), 316–319.
Scitovich, V.P., Lazarevich, L.M., 1985. Estimation of stress condition of rock massive by EMR. In: Smirnov, V. (Ed.), Geophysical Methods of Stress and Deformation Control. Novosibirsk, pp. 65–66 (in Russian).
Sobolev, G.A., Semerchan, A.A., Salov, B.G., 1982. Precursors of the destruction of large rock sample. Phys. Solid Earth 18 (8), 572–580.
Warwick, J.W., Stoker, C., Meyer, T.R., 1982. Radio emission associated with rock failure: possible application to the Great Chilean Earthquake of May 22,1960. J. Geophys. Res. 87 (b4), 2851–2859.
Yamada, I., Masuda, K., Mizutani, H., 1989. Electromagnetic and acoustic emission associated with rock fracture. Phys. Earth Planet. Inter. 57, 157–168.
Yoshino, T., Tomizawa, I., 1989. Observation of low-frequency electromagnetic emissions as precursors to the volcanic eruption at Mt. Mihara during November, 1986. Phys. Earth Planet. Inter. 57, 32–39.
Yoshino, T., Tomizawa, I., Sugimoto, T., 1993. Results of statistical analysis of low-frequency seismogenic EM emissions as precursors to earthquakes and volcanic eruptions. Phys. Earth Planet. Inter. 77, 21–31.
Zurkov, S.N., Kuksenko, V.S., Slutsker, A.I., 1969. Formation of submicroscopic cracks in polymers under load. Sov. Phys., Solid State 11 (2), 238–245.